



Feasibility of Integrating an MR Receive Coil Array into the MRcollar

Gennaro G. Bellizzi*⁽¹⁾, Kemal Sumser⁽¹⁾, Gerard C. van Rhoon⁽¹⁾, Ria Forner⁽²⁾, Margarethus M. Paulides^(1,3)

(1) Department of Radiation Oncology, Erasmus University Medical Center, Rotterdam, The Netherlands

(2) Department of Radiology, Utrecht Medical Center, Utrecht, The Netherlands

(3) Center for Care&Cure Technologies, Department of Electrical Engineering, Eindhoven University of Technology, The Netherlands

Abstract

Temperature monitoring is essential for a controlled application of hyperthermia in the head & neck to counteract the heterogeneous thermoregulation. Magnetic resonance (MR) thermometry can be used to monitor the 3D temperature pattern, so we are developing the world's first hyperthermia applicator for MR guided treatment of head & neck cancers. To maximize imaging signal-to-noise (SNR) but also allow an independent choice of the radiofrequencies for imaging and heating, our approach is based on integrating heating antenna- and imaging coil-arrays into one device. In this work, we developed and experimentally assessed the dual-function using a 3-channel receiver-only coil array designed for a 1.5T MR scanner (64 MHz) integrated into one of the two MRcollar shells containing six antennas operating at 434 MHz. Vector network analyzer measurements showed an average S_{ii} equal to -14dB and S_{ij} equal to -12dB with a 2cm geometric overlap. MR imaging experiments showed an average SNR improvement of +40dB when comparing the proposed coil to the conventional body coil. Results show the feasibility of the approach, and therefore paves the way for a clinical prototype for testing our dual-function approach in phantoms, volunteers and patients.

1 Introduction

During hyperthermia cancer therapy, the tumor is elevated to a supraphysiologic temperature (40-44°C) for a given time (60-90min). This is generally achieved using external electromagnetic field sources operating in the radiofrequency (RF) range. Clinical effectiveness of hyperthermia would benefit from achieving higher temperatures, which can be achieved by more target conformal heating [1]. Three-dimensional temperature monitoring is essential for real-time dosimetry that serves to adjust the heating settings. Such feed-back controlled heating is especially needed in the head & neck because of the unpredictable and heterogeneous thermoregulation [2]. However, conventional dosimetry is based on invasive interstitial thermometry probes, which often are infeasible, cause serious discomfort, pose infection risks and provide only a very limited spatial resolution [3]. Recently, magnetic resonance (MR) thermometry was shown as a promising tool for 3D non-invasive temperature monitoring during hyperthermia [4-6]. However, doubtful accuracy due to technological limitations impeded wide-

spread clinical application. This motivated us to design and prototype the MRcollar (Figure 1): the first MR compatible hyperthermia applicator for the head & neck.

However, MR thermometry accuracy is critically dependent on high signal-to-noise-ratio (SNR), which is achievable by minimizing the distance of the receiver coils to patient skin [7]. Therefore, we also are investigating the development of the next-generation dual-function hyperthermia applicator that integrates the MR coil array for imaging and the RF hyperthermia phased arrays for heating [8]. Hence two separate RF arrays are integrated into one single device: one for heating at 434MHz and one for imaging at the MR scanner's Larmor frequency. This integration allows an independent choice of the operating frequencies without compromising on heating quality, while still using commercially available MR scanner. Moreover, high SNR for accurate MR thermometry is aimed at by placing the receive coil array in close skin proximity.

The first step towards demonstrating our approach has been to prove the feasibility of applying hyperthermia with 12 patch antennas operating at 434MHz in a 1.5T MR scanner using the body coil for thermometry [9]. Following, an innovative Yagi-Uda antenna concept has been designed to further minimize the influence of the hyperthermia antennas on MR compatibility [10]. Finally, a preliminary demonstration of the dual-function operation has been shown using a reduced scale experimental setup [11]. However, the actual feasibility of integrating a multi-channel receiver-only coil array within our newly prototyped applicator was never been investigated. This is not a trivial task because of the very limited space (Figure 1) and hence its proper operation is not granted or accurately predictable by simulations. Experimentally demonstrating the feasibility of this integration is the next step towards further developments.

In this communication, we experimentally assess the feasibility of integrating a 3-channel receiver-only coil array within one of the two shells of the MRcollar (Figure 1). A tailored MR coil array has been designed and prototyped aiming at minimizing the required electronic circuitry. A vector network analyzer (VNA) has been used to characterize the prototype according to [12]. Finally, imaging performances have been assessed and benchmarked to the integrated body coil of a 1.5T MRI-scanner.

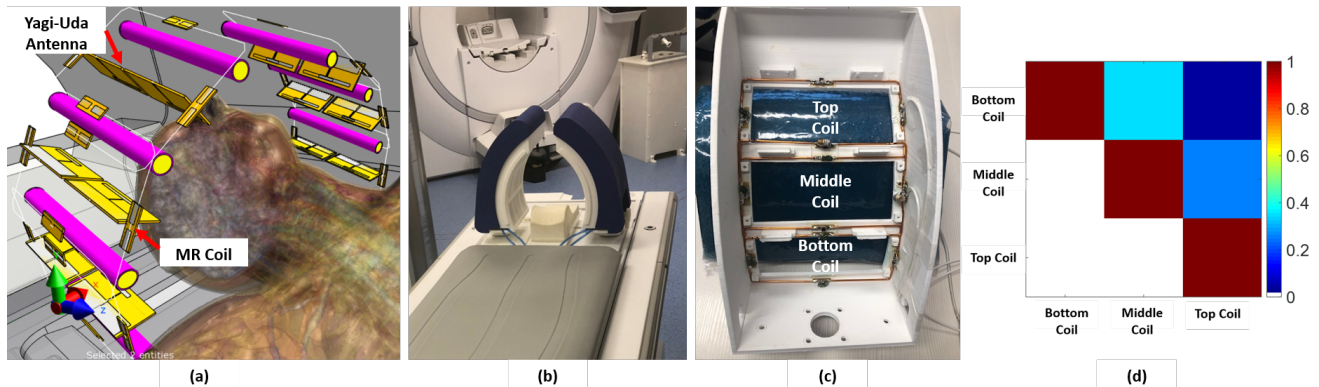


Figure 1. (a) Model of the MRcollar in Sim4Life. (b) Picture of the MRcollar on the MR table. (c) Picture of the 3-channel receiver-only coil array in place within the shell for the MRcollar without the antennas modules. (d) Noise correlation matrix of the 3-channel receiver-only coil array.

2 Materials & Methods

Integrating a multi-channel receiver-only coil array into the MRcollar is a challenging task as it requires electronics to be able to accommodate a very limited space (Figure 1), still surround the heating antennas to geometrical decouple from them. In addition, accurate MR thermometry requires high SNR as well as fast multi-channel imaging approach. As such, integration of existing commercial coils is unfeasible.

The prototyped coil array (Figure 1) is a 3-channel receive-only array and it consists of a bottom (15×8 cm), a central (15×12 cm) and a top (15×8 cm) rectangular shaped loop, fabricated using etched copper wire ($\varnothing=0.2$ cm) and copper PCBs for capacitor breaks. Coils were tuned and matched when placed on a 2cm-thick bag filled with deionized water bolus, which was placed on top of a muscle-equivalent phantom provided by the MR vendor. This is a good estimate of the actual final setup.

Each coil was tuned to 63.89MHz using both fixed and tuning capacitors (ATC multi-layer ceramic 100B/TN series) with an additional matching network at the feed port. Coils were connected to a 100cm (Habia RG174, 50 Ohm, silver-plated copper) coaxial cable at the feed port. Geometric overlap was used to minimize coupling, S21, between elements in the array.

Decoupling from the transmit coil has been achieved by means of an active and a passive diode detuning circuit [12]. These circuits were implemented by placing the diode (MA4P7461F-1072T, UMX9989AP) in parallel with tuning capacitor to achieve adequate decoupling level. In the final setup, the detuning performance was assessed by switching the diode on and off using an external power supply and measuring the S21 between the two states.

First, the noise correlation matrix was measured using the MR scanner to investigate the decoupling level between the coils [12]. Second, local static magnetic field artifacts have been investigated by measuring the B0 map in presence and absence of the coil using the body coil with a spoiled RF Gradient Echo sequence (TR=50ms, Flip Angle=15°, Image Matrix=256x256, Read out Bandwidth=31.25kHz, FOV=25.6, Slice thickness=0.1 cm). Third, the proper operation of the detuning circuits has

been investigated by measuring the B1 map in presence and absence of the coil using the body coil applying a Bloch-Siegert Shift (TR=28ms, TE=12.4ms, Flip Angle=15°, Image Matrix=128x128, Read out Bandwidth=31.25kHz, FOV=25.6, Slice thickness=0.1 cm) [13].

Finally, SNR was measured using imaging by a GE 450w 1.5T and the 3-channel coil array as compared to the body coil. The prototype coil array was placed on the one side of a DQA HD/SNR phantom including different shapes and objects (model 2321554, GE Medical Systems - MR Division, Waukesha, WI). The SNR was calculated at two region of interest (ROI) centered at 2cm (ROI₁) and 5cm (ROI₂) in the phantom, as shown in Figure 2. A Spoiled Gradient Echo sequence has been used with the following parameters flip angle=21°, FOV= 50, TE=4.5ms, TR=100ms, and 0.2cm voxel size.

3 Results & Discussion

The measured reflection coefficient of the 3-channel receiver-only coil array was -14 ± 2 dB (range -11 to -17dB) whereas a decoupling of -12 ± 4 dB (range -9.5 to -18dB) has been achieved through geometric overlap of 2cm. This is close to what predicted in the MRcollar simulation-guided design [14]. However, coil decoupling is highly sensitive and depending on many factors including coil material, shape and load. Loops have shown an average unloaded quality factor of 220 (range 220 to 240) and a loaded of 103 (range 90 to 120) giving an adequate ratio according to [12].

The noise correlation matrix depicted in Figure 1(d) identifies a decoupling level <0.3 between the three resonant loops. Absence of local static magnetic field artifacts has been assessed. The comparison between the flip angle maps when in presence and in absence of the receive coil array has shown a deviation lower than 2%, which proves the proper functioning of the coil array [12].

Figure 2 depicts the magnitude images acquired when using either the 3-channel coil array or the body coil as receiver. The two different ROIs have been reported. Results show that the SNR levels achieved using the 3-channel coil are always higher than the one achieved using the body coil both for ROI₁ and ROI₂. Results showed

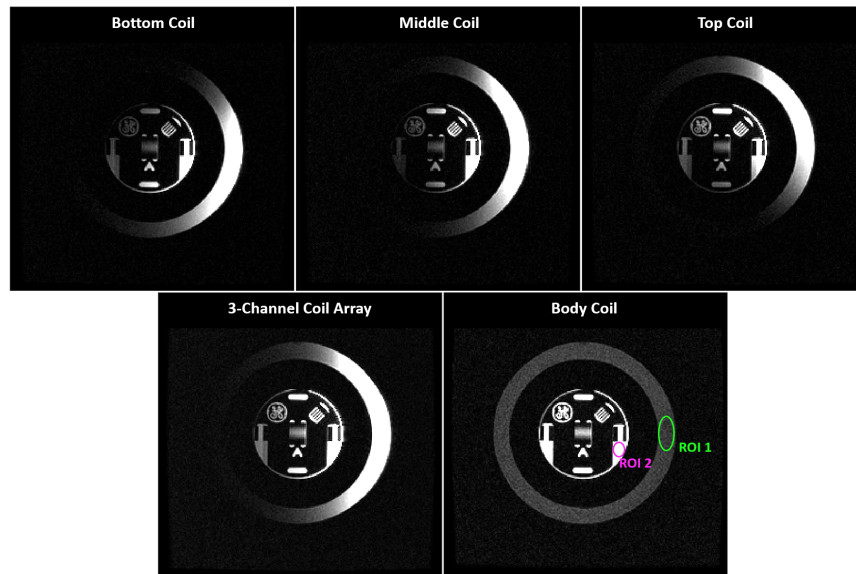


Figure 2. Comparison of magnitude images acquired using either the integrated 3-channel coil or the body coil as receiver. Two ROIs are centered at 2cm and 5cm, respectively ROI₁ and ROI₂ within the phantom surface and are marked in green and magenta, respectively.

+65dB and +20dB SNR improvement, respectively for ROI₁ and ROI₂, when using the 3-channel coil array as compared to the body coil.

4 Conclusions

The results of our investigation experimentally validate the feasibility of integrating a 3-channel receiver-only coil array for a 1.5T MR scanner (64 MHz) within one shell of the MRcollar (operating at 434 MHz). The prototype coil array was shown to be properly matched ($S_{ii}=-14\text{dB}$) and decoupled ($S_{ij}=-12\text{dB}$) both through bench measurements and MR imaging experiments, and it was shown to be compliant with standard safety regulation [11]. Also, our results demonstrate an improvement of the SNR (+40dB on average) when using the 3-channel prototype instead of the body coil. The results of this communication are the last necessary step towards the final development of our next generation dual-function integrated approach to MR-guided hyperthermia that will enable truly simultaneous dual-function operation

5 References

1. Sherar, M., et al., *Relationship between thermal dose and outcome in thermoradiotherapy treatments for superficial recurrences of breast cancer: data from a phase III trial*. International Journal of Radiation Oncology* Biology* Physics, 1997. **39**(2): p. 371-380.
2. Paulides, M.M., G.M. Verduijn, and N. Van Holthe, *Status quo and directions in deep head and neck hyperthermia*. Radiation Oncology, 2016. **11**(1): p. 21.
3. van der Zee, J., et al., *Practical limitations of interstitial thermometry during deep hyperthermia*. International Journal of Radiation Oncology* Biology* Physics, 1998. **40**(5): p. 1205-1212.
4. Winter, L., et al., *Magnetic resonance thermometry: methodology, pitfalls and practical solutions*. International Journal of Hyperthermia, 2016. **32**(1): p. 63-75.
5. Curto, S., et al., *Quantitative, Multi-institutional Evaluation of MR Thermometry Accuracy for Deep-Pelvic MR-Hyperthermia Systems Operating in Multi-vendor MR-systems Using a New Anthropomorphic Phantom*. Cancers, 2019. **11**(11): p. 1709.
6. Poorter, J.D., et al., *Noninvasive MRI thermometry with the proton resonance frequency (PRF) method: in vivo results in human muscle*. Magnetic resonance in medicine, 1995. **33**(1): p. 74-81.
7. Kulkarni, M.V., J.A. Patton, and R.R. Price, *Technical considerations for the use of surface coils in MRI*. American Journal of Roentgenology, 1986. **147**(2): p. 373-378.
8. Adibzadeh, F., et al., *Systematic review of pre-clinical and clinical devices for magnetic resonance-guided radiofrequency hyperthermia*. International Journal of Hyperthermia, 2020. **37**(1): p. 15-27.
9. Paulides, M.M., et al., *Laboratory prototype for experimental validation of MR-guided*

- radiofrequency head and neck hyperthermia*. *Physics in Medicine & Biology*, 2014. **59**(9): p. 2139.
10. Paulides, M.M., et al., *A printed Yagi–Uda antenna for application in magnetic resonance thermometry guided microwave hyperthermia applicators*. *Physics in Medicine & Biology*, 2017. **62**(5): p. 1831.
 11. Bellizzi, G.G., et al. *Characterization of an Integrated Radiofrequency System for MR-guided Hyperthermia*. in *2010 14th European Conference on Antennas and Propagation (EuCAP), 1-4*. 2020.
 12. Hoffmann, J., et al., *Safety testing and operational procedures for self - developed radiofrequency coils*. *NMR in Biomedicine*, 2016. **29**(9): p. 1131-1144.
 13. Sacolick, L.I., et al., *B1 mapping by Bloch - Siegert shift*. *Magnetic resonance in medicine*, 2010. **63**(5): p. 1315-1322.
 14. Paulides, M.M., et al., *Novel applicator design for MR guided RF hyperthermia in head and neck cancers: heating performance and RF coupling*, in *SMRT, 27th Annual Meeting Joint ISMRM and ESMRMB*. 2018.